RSC Advances

PAPER

View Article Online
View Journal | View Issue

Cite this: *RSC Adv.*, 2025, **15**, 10511

Bio-based cellulose benzenesulfonic acid-catalyzed dehydration of fructose to 5-hydroxymethylfurfural†

Aniwat Pengsawang,[a] Atthapon Srifa [b] and Vorranutch Itthibenchapong *[a]

In this work, cellulose benzenesulfonic acid (CBSA) was successfully prepared by chemically modifying cellulose with a 4-chlorobenzenesulfonic acid reagent in toluene, providing mainly Brønsted acid sites, as determined by pyridine-DRIFT, for use as a potential solid acid catalyst. The as-prepared CBSA was characterized by various techniques, and its catalytic performance for the conversion of fructose to 5-HMF was examined in dimethyl sulfoxide. In particular, the effects of reaction temperature and reaction time on its activity were investigated. The results showed that CBSA with a 10 wt% loading exhibited the highest catalytic activity, achieving a fructose conversion of 100% and a 5-HMF yield of approximately 85% when a reaction temperature of 140 °C and a reaction time of 180 min were employed. The reusability of CBSA was moderately satisfactory. A 5-HMF yield of 55% and a fructose conversion of 97% were obtained after a total of 4 runs (3 reuse cycles). According to the XPS results of the spent catalyst, the decrease in catalytic performance was mainly due to the insufficiency or loss of the $-SO_3H$ group as the active site for the catalytic dehydration of fructose. These findings could be beneficial for advancing heterogeneous catalysis in saccharide valorization and the development of bio-based solid Brønsted acid catalysts.

Received 4th December 2024
Accepted 22nd March 2025

DOI: 10.1039/d4ra08540j

rsc.li/rsc-advances

1. Introduction

Most of the chemicals and fuels utilized today for various activities, such as manufacturing products and transportation, have been derived from petroleum *via* refinery processes. However, due to the high global demand for energy and products, as well as the decline in oil and natural gas resources, the production of chemicals and fuels from alternative sources, specifically renewable feedstocks, is urgently needed.[1,2] Carbohydrates, including fructose, glucose, sucrose, and cellulose, are considered attractive alternative starting materials for the production of high-value-added biochemicals and biofuels, such as 5-hydroxymethylfurfural (5-HMF),[3–6] 5-ethoxymethylfurfural (EMF),[1] and 2,5-dimethylfuran (DMF).[7] Among these, in terms of high sustainability, cellulose is a particularly strong candidate, as it is the most naturally abundant organic molecule on Earth. Cellulose is a linear-chain biopolymer composed of thousands of D-glucose residues linked by β-(1 → 4) linkages.[8] It is found primarily in plants as the main constituent of the plant cell wall.[9] Over the past century, research on the properties of cellulose and its derivatives, as well as their applications, has been extensively conducted. Cellulose itself can be utilized as a starting material for the synthesis of many high-value-added biochemicals, such as levulinic acid,[10] butyl levulinate,[11] light aromatics,[12] and furans.[12–14] Moreover, cellulose in various forms, such as hydrogel and nanocellulose, has been used as a support for nanoparticles or as a catalytic complex molecule.[15,16] Additionally, cellulose can form composites with photoactive compounds, such as Fe_3O_4, for application in photocatalytic degradation.[17] Apart from being utilized as a support for catalytically active materials, cellulose with some degree of substitution (DS) has also demonstrated catalytic activity for a variety of chemical reactions. For instance, Liu *et al.* demonstrated that cellulose sulfuric acid could catalyze the etherification of 5-HMF to form 5-ethoxymethylfurfural (EMF) in ethanol, achieving a high EMF yield of 84.4% under optimized reaction conditions.[18] Nasseri *et al.* employed a CSA solid acid catalyst to regioselectively synthesize pyrazoles from hydrazines/hydrazides and 1,3-diketone molecules in water *via* the Knorr synthesis and reported high yields of the target pyrazoles.[19] In 2015, Daneshfar and Rostami reported the development of a simple catalytic process based on a cellulose sulfonic acid solid catalyst for the synthesis of 5-membered carbo- and heterocycles. The results showed that cellulose sulfonic acid could catalytically transform unactivated dienones and α,β-

[a]*National Nanotechnology Center (NANOTEC), National Science and Technology Development Agency (NSTDA), Pathum Thani 12120, Thailand. E-mail: vorranutch@nanotec.or.th*

[b]*Department of Chemical Engineering, Faculty of Engineering, Mahidol University, Nakhon Pathom 73170, Thailand*

† Electronic supplementary information (ESI) available. See DOI: https://doi.org/10.1039/d4ra08540j

unsaturated hydrazones into cyclopentenoids and pyrazolines, respectively, *via* cyclization reactions with excellent product yields.[20]

The acid-catalyzed dehydration of fructose to 5-HMF has attracted attention from both academic and industrial sectors.[21] This is because 5-HMF is one of the most important platform chemicals for the synthesis of biofuels and biochemicals. Also, fructose in its fructofuranose form is highly selective for 5-HMF formation.[22,23] Acid catalysts with Brønsted acid sites are essential for this reaction. Compared with their homogeneous counterparts, heterogeneous acid catalysts with Brønsted acid sites can be more easily reused and separated from reaction mixtures. Therefore, many attempts to develop highly active solid acid catalysts with Brønsted acid sites, especially from renewable sources, such as biomass or biomass-derived compounds, have been made.[24–36] Liu *et al.* reported the use of cellulose sulfuric acid as a catalyst for 5-HMF synthesis from fructose. They obtained an impressive 5-HMF yield of 93.6% from experiments conducted at 100 °C for 45 min in DMSO with a 28 wt% catalyst loading.[18] Liu *et al.* also prepared sulfonated carbonaceous materials (SAC-4-*X*-SO_3H) from glucose, benzyl chloride, and concentrated sulfuric acid and examined the catalytic activity of the synthesized materials for fructose dehydration to 5-HMF. They found that at a reaction temperature and time of 130 °C and 1 h with 0.25 g of SAC-4-2-SO_3H (50 wt% catalyst loading) in an acetone–DMSO mixture, a 5-HMF yield of 90% could be obtained.[27] Li *et al.* also investigated the catalytic activity of the carbon-based LCSA-900 catalyst in DMSO for fructose conversion to 5-HMF, and reported a fructose conversion of 98% and 5-HMF yield of 75.7% could be achieved at 170 °C with a catalyst dosage of 150 wt%.[33] Sulfonated solid acid catalysts from various biomass materials, *e.g.*, cotton gin trash (CGT),[28] plant leaves,[32] and pine needle,[36] have reportedly shown promising activities, with 5-HMF yields of 80%, 93%, and 96%, respectively, under the respective optimal reaction conditions. Apart from sulfonated catalysts, the carbon-based catalyst with only a carboxyl (–COOH) functional group on the surface, denoted as LDMCC-900, also exhibited catalytic activity for the conversion of fructose to 5-HMF,[24] and a 5-HMF yield of 74.3% was obtained when DMSO was used as a solvent and the reaction was performed at 140 °C with a catalyst loading of 10 wt%.

It can be seen that the majority of solid acid catalysts based on renewable sources for the conversion of fructose to 5-HMF are produced through carbonization, which typically requires high temperatures, and sulfonation with corrosive sulfuric acid. The direct utilization of natural abundant materials, such as cellulose, to produce sulfonated catalysts by chemical functionalization with reagents containing a sulfonic acid group could substantially reduce the consumption of fossil-based energy and the need for the use of highly corrosive sulfonating agents. Research work conducted by Li *et al.* into the application of benzenesulfonic acid-functionalized biochar (biochar-$PhSO_3H$) as a solid acid catalyst for the esterification of oleic acid with methanol and alkylation of 4-ethylphenol with benzyl alcohol showed that the biochar-$PhSO_3H$ catalyst outperformed the traditional sulfonated biochar (biochar-SO_3H) catalyst for both reactions,[37] suggesting that the benzenesulfonic acid group could potentially be an alternative to the sulfo group for acid-catalyzed reactions. This suggests it would be worth exploring the use of benzenesulfonic acid-based solid catalysts for the catalytic conversion of fructose to 5-HMF.

Although numerous articles have been published on fructose conversion to 5-HMF catalyzed by solid Brønsted acid catalysts, to the best of our knowledge, there has been no report yet on the use of cellulose benzenesulfonic acid as a catalyst for this conversion. In this work, a novel acid derivative of cellulose, referred to as cellulose benzenesulfonic acid (CBSA), was synthesized from microcrystalline cellulose powder and 4-chlorobenzenesulfonic acid dissolved in toluene and used as the catalyst for the conversion of fructose to 5-HMF. The CBSA product was characterized by spectroscopic and microscopic techniques to gain insights into its physicochemical properties. NMR, FTIR, and PXRD were employed to elucidate the structure and determine the constituents of CBSA. The thermal stability of CBSA under an inert atmosphere was investigated by TGA. The number of sulfonic groups (–SO_3H) was determined by sulfur analysis and acid–base titration following the H^+–Na^+ ion exchange. Additionally, the morphology and specific surface area of CBSA were analyzed by SEM and Brunauer–Emmett–Teller (BET) surface area analysis. The catalytic activity of the as-synthesized CBSA material with a 10 wt% loading for the conversion of fructose to 5-HMF was demonstrated in a monophasic DMSO solvent system at different reaction temperatures (100–140 °C) and reaction times (45–180 min). Under the optimal reaction conditions, the recyclability of CBSA and the characteristics of the spent catalyst after 4 batch runs were investigated.

2. Experimental section

2.1 Materials

All the chemicals were used as received without further purification and included Avicel PH-101 microcrystalline cellulose (Sigma-Aldrich), toluene (AR grade, RCI Labscan), 4-chlorobenzenesulfonic acid (TCI), ethyl alcohol (Absolute (Denatured), GR grade), fructose (Sigma-Aldrich, ≥99%), and DMSO (RCI Labscan, AR grade).

2.2 Synthesis of cellulose benzenesulfonic acid (CBSA)

The synthesis procedure was adapted from a previous method reported by Zhang *et al.*[38] First, the Avicel PH-101 microcrystalline cellulose powder (CMC) of *ca.* 2.1 g was added into a round-bottom flask. Next, 140 mL of toluene was added and then the mixture was stirred at room temperature for 15 min with a rotational speed of 500 rpm. Then, approximately 2.1 g of 4-chlorobenzenesulfonic acid was mixed with the cellulose suspension under stirring at room temperature for 1 h. The obtained mixture was further stirred at 500 rpm under reflux for 8 h at 115 °C. After that, the mixture was left to cool to room temperature and then filtered. The separated solid product was washed with hot toluene and ethanol until the pH of the filtrate was about the same as that of ethanol. The obtained catalyst

powder was finally dried at 60 °C overnight under a vacuum atmosphere. The dried cellulose benzenesulfonic acid catalyst was denoted as CBSA.

2.3 Characterization of the CBSA catalyst

The functional groups of CBSA were confirmed by Fourier-transform infrared spectroscopy (FTIR) analysis using a Nicolet iS50 FTIR Spectrometer (Thermo Fisher Scientific) in the transmission mode. The spectra were collected in the wavenumber range of 400–4000 cm^{-1} with a resolution of 4 cm^{-1}. Before the measurements, the CBSA sample was homogeneously mixed with KBr powder through grinding and the mixture was pelletized under a pressure of 2 tons for 3 min. Identification of the phase and crystalline structure of the cellulose was performed by powder X-ray diffraction (PXRD) using a Bruker D8 diffractometer utilizing CuKα radiation. The data were collected in the 2θ range of 5–80° with a time step of 0.5 s and an increment of 0.020°. The morphology and particle-size distribution of CBSA were studied by field emission scanning electron microscopy (FE-SEM, SU8200, Hitachi). The average particle size ($N = 30$) was determined using ImageJ software. The specific surface areas of the CBSA and CMC samples were measured by the N_2 sorption technique at 77 K (Quantachrome Instruments) and the collected data were analyzed using the Brunauer–Emmett–Teller (BET) method. The thermal stability of the samples was studied by thermogravimetric analysis (TGA) performed on a Mettler Toledo TGA/DSC 3+ instrument under a N_2 atmosphere from 30 °C to 900 °C with a heating rate of 10 °C min^{-1} and a N_2 flow rate of 40 mL min^{-1}. The sulfur content of all samples was measured using a Leco 628S sulfur analyzer. XPS analysis was performed on the samples using an AXIS Supra spectrometer (KRATOS Analytical) with an Al X-ray source (225 W). All the collected XPS data were processed by CasaXPS software.[39] Chemisorption experiments, namely pyridine adsorption-diffuse reflectance infrared Fourier transform (Py adsorption-DRIFT), were conducted to study the types of acid sites of the CBSA catalyst. Here, Py adsorption on a pretreated CBSA sample was carried out at 140 °C. After 1 h, the physisorbed pyridine was evacuated for 1 h before the FTIR spectrum was collected under vacuum at the same temperature. The spectrum of CBSA collected at 140 °C under vacuum was employed as a background file for reprocessing the previously obtained spectrum. The FTIR analysis was performed on a Nicolet iS50 FT-IR spectrophotometer. All the collected data were processed using OMNIC spectroscopy software. Nuclear magnetic resonance (NMR) spectroscopy was used to determine the molecular structure of CBSA. Here, a certain amount of CBSA was first dissolved in DMSO-d_6 with stirring. The acquired solution was then loaded into a 500 MHz NMR spectrometer (UltraShield™ Bruker Avance III HD) and the ^1H as well as ^{13}C and 2D-HMBC spectra of the CBSA solution were recorded at ambient temperature (~23 °C) in water suppression mode. An energy dispersive X-ray fluorescence spectroscopy (μ-EDXRF spectrometer, 2 mm X-ray beam size, Orbis PC) was employed to determine the elemental composition of CBSA. Acid–base titration was also conducted for quantitative analysis of the sulfonic groups (–SO_3H) of the as-synthesized CBSA samples. Here, *ca.* 30 mg of the CBSA sample was transferred to a 100 mL Erlenmeyer flask. Then, 20 mL of 0.2 M sodium chloride solution was added into the flask and the mixture was stirred (250 rpm) at room temperature for 4 h. After that, the mixture was further sonicated for 1 h under temperature control (not exceeding 30 °C). The suspended solid was then filtered and the obtained filtrate was titrated with 0.01 M sodium hydroxide solution standardized with potassium hydrogen phthalate (KHP). The number of –SO_3H groups was calculated using the following equation:[40]

$$D_{-SO_3H}\ \left(\text{mmol } g_{\text{sample}}^{-1}\right) = \frac{C(OH^-) \times \Delta V}{m} \quad (1)$$

where D_{-SO_3H} is the density of –SO_3H groups on the surface of CBSA in mmol g^{-1}, $C(OH^-)$ is the concentration of NaOH solution (M), ΔV is the volume of NaOH solution used for the neutralization (mL), and m is the sample weight (g).

2.4 Catalytic activity test

The catalytic activity of CBSA for the conversion of fructose to 5-HMF was examined in a 100 mL stainless steel stirred tank reactor (STR) lined with a glass liner. In preparation for a typical reaction test, *ca.* 1.8 g of fructose was charged into a glass liner, and then 30 mL of DMSO was added. Upon the complete dissolution of fructose, 10 wt% CBSA with respect to the weight of fructose was dispersed under a stirring rate of 500 rpm at room temperature for 15 min. The mixture-containing glass liner was then loaded into the reactor. The reactor was purged with N_2 gas 3 times to remove air and then pressurized to 5 bar N_2 prior to the activity testing. The reaction mixtures were continuously stirred and heated to the desired temperature (100 °C, 120 °C, and 140 °C) at a heating rate of approximately 4 °C min^{-1} and held there for set periods of reaction time (45, 120, and 180 min). At the end of the reaction test, the reaction mixtures were cooled to room temperature and discharged to a filtration unit to separate out the spent CBSA catalyst. The obtained filtrate was filtered using a Nylon 0.2 μm syringe filter. Then, the liquid sample was analyzed by high-performance liquid chromatography (HPLC) using a Shimadzu LCMS-2020 instrument equipped with an Agilent Hi-Plex H 300 × 7.7 mm column. The HPLC analysis conditions were as follows: 5 mM H_2SO_4 as a mobile phase, a flow rate of 0.6 mL min^{-1}, an oven temperature of 45 °C, and RI and PDA at 320 nm for the detection of fructose and 5-HMF, respectively. The external standard calibration method was applied to quantify the amount of fructose remaining and 5-HMF produced. The conversion of fructose, yield of 5-HMF, and selectivity of 5-HMF were determined by the following equations.

$$\text{Fructose conversion } (\%) = \frac{\text{total number of moles of reacted fructose}}{\text{total number of moles of fructose}} \times 100 \quad (2)$$

$$\text{5-HMF yield } (\%) = \frac{\text{total number of moles of 5-HMF produced}}{\text{total number of moles of fructose}} \times 100 \quad (3)$$

$$\text{5-HMF selectivity } (\%) = \frac{\text{total number of moles of 5-HMF produced}}{\text{total number of moles of reacted fructose}} \times 100 \quad (4)$$

2.5 Reusability test

The reusability test for the CBSA catalyst was investigated at the reaction temperature of 140 °C for 180 min. In each run, the spent CBSA catalyst was separated and washed with ethanol under stirring. The obtained solid sample was subsequently vacuum dried at 60 °C for 15 h before the next run or additional characterization.

3. Results and discussion

3.1 Catalyst synthesis and characterization

The synthesis of cellulose benzenesulfonic acid (CBSA) yielded a black powder product with a yield of *ca.* 64% relative to the mass of the starting cellulose. To propose the structure of CBSA, the probable reactions between 4-chlorobenzenesulfonic acid and CMC under the employed synthesis conditions need to be

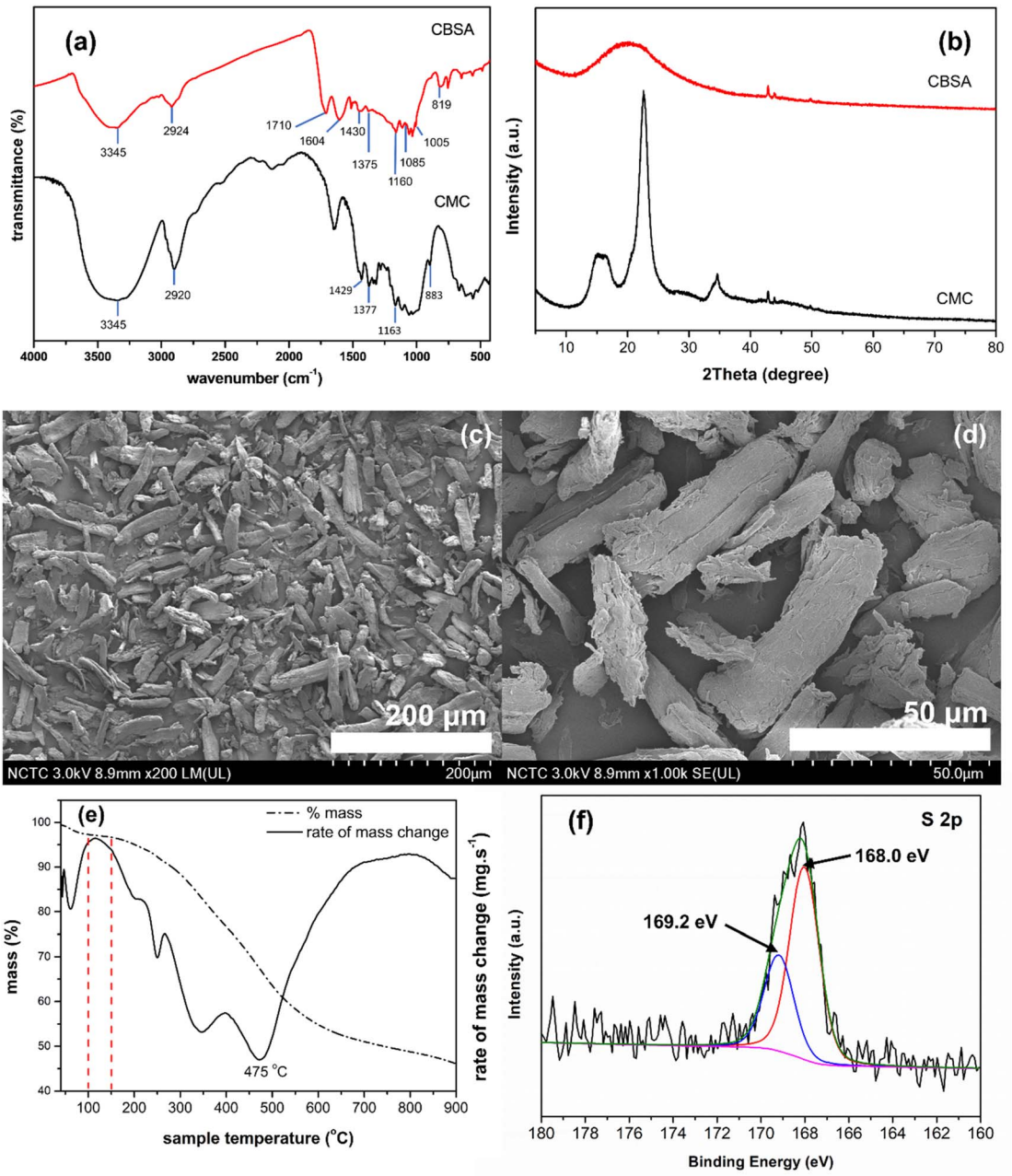

Fig. 1 Catalyst characterization: (a) FTIR spectra of cellulose microcrystals (CMC) and cellulose benzenesulfonic acid (CBSA), (b) PXRD patterns of CMC and CBSA, (c) SEM image of CBSA at 200× magnification, (d) SEM image of CBSA at 1000× magnification, (e) TGA profile of CBSA and, (f) XPS spectrum of CBSA in the S 2p region.

considered. The molecular structure of 4-chlorobenzenesulfonic acid contains a sulfo or $-SO_3H$ functional group in the *para* position relative to a chlorine atom. The sulfo group is a strongly deactivating group, which removes electron density from the adjacent π system *via* a resonance effect, resulting in reduced nucleophilicity of the benzene ring and the formation of a resonance structure with a positive charge on the carbon atom covalently bonded to Cl. Such a carbon is likely to be attacked by a nucleophile. It is widely known that aromatic molecules consisting of a benzene ring with a strong electron-withdrawing group and a halogen atom directly opposite to it are likely to undergo nucleophilic aromatic substitution at the C–X position, as the electron-withdrawing group can stabilize the carbanion formed. Since CMC contains nucleophilic hydroxyl functional groups, the nucleophilic aromatic substitution of –OH with 4-chlorobenzenesulfonic acid at the *para* position relative to the sulfo group to form $-O-PhSO_3H$ could have occurred. The hydroxyl group of the $-C^6H_2OH$ moiety is most likely a reaction site due to its minimal steric hindrance. The acid-catalyzed esterification of 4-chlorobenzenesulfonic acid and the $-C^6H_2OH$ moiety of the glucopyranose unit to form a sulfonic ester could also have occurred. This conclusion was drawn because the toluene solution of 4-chlorobenzenesulfonic acid at the reaction temperature was acidic. The FTIR and solution-state NMR results were also taken into account. The collected FTIR spectrum of CBSA, as shown in Fig. 1a, was closely similar to that of CMC, with the appearance of IR absorption peaks at *ca.* 3345, 2920, 1429, 1377, and 883 cm^{-1}, characteristic of native cellulose.[41] These peaks were attributed to the stretching vibration of a hydrogen bond of the –OH group, C–H stretching vibration, intermolecular hydrogen bonding at the $C^6(-C^6H_2-OH)$ group, asymmetric stretching of C–H bonds, and glycosidic-C_1–H deformation. An absorption peak centered at 1163 cm^{-1}, corresponding to the stretching vibration of a C–O–C glycosidic linkage, was also observed.[42–45] Moreover, three additional peaks at 819, 1005, and 1085 cm^{-1}, attributed to S–O symmetric stretching, S–O asymmetric stretching, and O=S=O symmetric stretching,[37,46] respectively, were present in the FTIR spectrum of CBSA, indicating the successful functionalization of cellulose with the $-S(=O)_2O-$ containing groups. Under the reaction conditions for CMC derivatization, the $-CH_2OH$ or –OH groups of cellulose could have undergone oxidation to some extent, as evidenced by the IR absorption peak at 1710 cm^{-1}, which was associated with the C=O stretching vibration of carboxylic acid or ketone functional groups.[47]

Next, solution-state NMR spectroscopy in 2D mode was employed to determine the molecular structure of CBSA. The heteronuclear multiple bond correlation (HMBC) experiment, which gives correlations between carbon and hydrogen atoms separated by 2, 3, or sometimes 4 bonds in conjugated systems, was conducted, and the results are shown in Fig. S1.† A correlation between the proton corresponding to a chemical shift of *ca.* 3.56 ppm (proton in red) and the carbon corresponding to a chemical shift of *ca.* 139 ppm (carbon in red) was observed. According to Sasaki *et al.*, the ^1H signal at approximately 3.56 ppm could be assigned to the hydrogen atoms directly attached to the 6th carbon of internal and terminal reducing glucose residues.[48] The ^{13}C signal at *ca.* 139 ppm could be assigned to the carbon of the substituted benzene. The low intensity of this peak could be due to a small amount of the corresponding *ipso* carbon species. Experimentally, the results from the NMR measurements, including ^1H, ^{13}C, 2D-HSQC, and 2D-HMBC, of the 4-chlorobenzenesulfonic acid in DMSO-d_6 solution, pointed out that the ^{13}C signals at 133.4 and 146.9 ppm were associated with the carbon atoms directly bonded to chlorine and the $-SO_3H$ group, respectively. Thus, the peak appearing at *ca.* 139 ppm in the ^{13}C NMR spectrum of CBSA could be attributed to the benzene ring carbon bonded to a group of atoms with a higher electron-attracting ability than chlorine but lower than the $-SO_3H$ group. The $-C^6H_2O-$ group satisfied these conditions. Accordingly, it is probable that the $-C^6H_2OPhSO_3H$ moieties were present in CBSA. Based on the considerations and experimental results above, a possible structure of CBSA was proposed, as depicted in Fig. 2. After CBSA was treated in a NaCl aqueous solution under stirring and sonication, the number of proton sites, as determined by acid–base titration, was 0.21 mmol g^{-1}. This result indicated the exchange of Na^+ and H^+ of the sulfo group, confirming its presence in CBSA.

The crystalline structure of CBSA was studied by XRD. The XRD pattern of pristine CMC (starting material) displayed diffraction peaks at $2\theta = 15°$, 17°, and 22.5°, which were associated with the $(1\bar{1}0)$, (110), and (200) diffractions (Fig. 1b). These peaks are characteristic of cellulose I.[49,50] The small peaks appearing at $2\theta = 43°$, 44°, and 50° in both the XRD patterns of CMC and CBSA were from the glass XRD sample holder. The XRD pattern of CBSA showed a single broad peak centered at $2\theta = 20°$, indicating lower crystallinity of CBSA compared to CMC, with a higher degree of the amorphous phase. This phase transformation could be caused by a reduction in the intra- and intermolecular hydrogen bonds during functionalization.[51] Fig. 1c and d show the FE-SEM images at two different magnifications of the CBSA sample. It could be seen that the majority of the particles were blade-like or rod-like in shape, with an average length and width of 59 ± 18 μm and 18 ± 4 μm, respectively. The BET specific surface area of CBSA was 6.1 $m^2\ g^{-1}$, which was slightly higher than that of CMC (2.1 $m^2\ g^{-1}$).

To study the thermal stability of CBSA, thermogravimetric analysis (TGA) under a N_2 atmosphere was employed. A mass loss in the temperature range of 30–100 °C was observed in the thermogram of CBSA (Fig. 1e). This loss could be ascribed to the removal of adsorbed water molecules from the analyzed sample.[52] CBSA remained thermally stable up to *ca.* 150 °C, as indicated by the minimal mass change between 100 °C and 150 °C. A considerable mass loss of about 47% was observed between 150 °C and 700 °C, with the highest rate of mass change occurring at 475 °C. This mass loss could be associated with the decomposition of the cellulose and benzenesulfonic acid groups.

The CBSA catalyst was also investigated by XPS analysis to confirm the presence of sulfonate groups in its structure. The S 2p XPS spectrum of CBSA is displayed in Fig. 1f. Deconvolution of the S 2p profile yielded a single spin–orbit doublet centered at

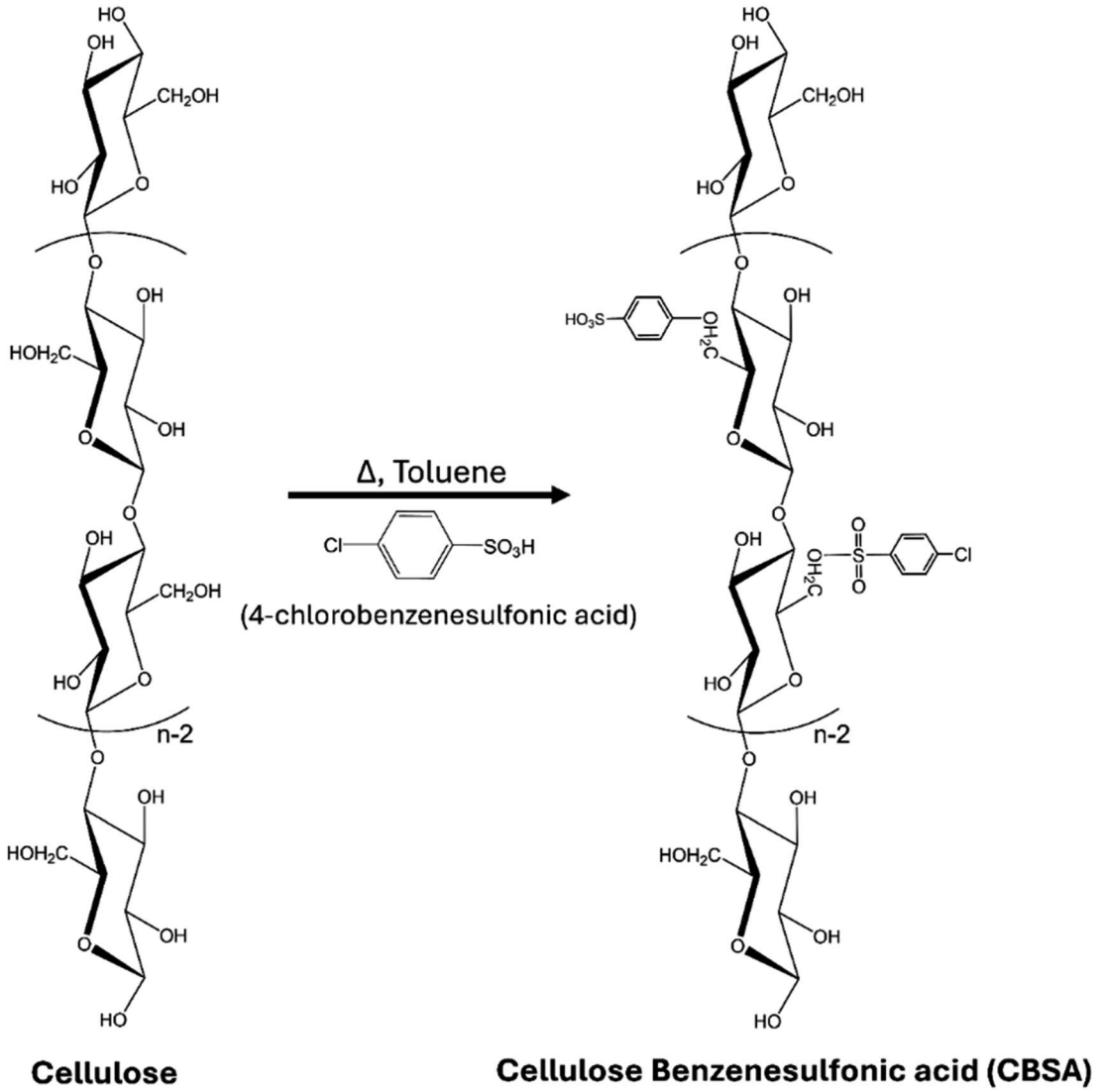

Fig. 2 Chemical synthesis and proposed structure of cellulose benzenesulfonic acid (CBSA).

168.0 eV (S $2p_{3/2}$) and 169.2 eV (S $2p_{1/2}$), which was attributed to the sulfonic (–SO_3H) group,[53–55] confirming the presence of –SO_3H moieties in the as-prepared CBSA solid catalyst. Detailed analyses of the C 1s and O 1s spectra for CBSA can be found in Fig. S2a, b and Table S1.† The Cl 2p peak was also observed. The binding energy of 200.7 eV for the $2p_{3/2}$ core-level electrons, acquired from the deconvolution (see Fig. S2e†), were ascribed to chlorine atoms covalently bonded to sp^2 carbon,[56,57] verifying the existence of the –C^6H_2O–S(=O)$_2$PhCl groups from the esterification in CBSA.

The total sulfur content of CBSA was determined by sulfur elemental analysis, which was typically used to quantitatively measure sulfur content in solid catalyst samples. As demonstrated in the work of Liu *et al.*, they prepared a cellulose sulfuric acid (cellulose-SO_3H) catalyst and determined its sulfur content using elemental analysis. The results showed that the as-synthesized catalyst contained 0.56 mmol of S per gram of catalyst. They also conducted an acid–base titration of a solution obtained by dispersing cellulose-SO_3H in 0.1 M KCl aqueous solution under stirring to determine the number of H^+ sites. Since this methodology involved the exchange of K^+ and H^+ of the sulfo group, the determined number of H^+ sites was equivalent to the number of –SO_3H groups and, thus, to the moles of S. The number of H^+ sites was determined to be 0.54 mmol per gram of catalyst, which was relatively close to the sulfur content. According to these results, it was concluded that most of the sulfur species in the cellulose sulfuric acid catalyst existed in the form of –SO_3H.[18] In our work, it was found that CBSA contained 0.37 mmol of S per g of CBSA, as determined using a total sulfur analyzer. However, the number of H^+ sites in CBSA, determined by a similar acid–base titration as described above, was 0.21 mmol g^{-1} of CBSA, which was significantly different from the total sulfur content. Therefore, these findings indicated that the sulfur species present in CBSA were not only in the form of benzenesulfonic acid groups but also existed in other forms.

The type of acidity in CBSA was qualitatively investigated by Py adsorption-DRIFT experiments, as presented in Fig. S3.† The IR absorption peaks at 1457, 1488, and 1541 cm^{-1} were observed in the Py adsorption-DRIFT spectrum of CBSA. The band at 1457 cm^{-1} was attributed to Lewis acid sites originating from the S=O double bonds of the $-SO_3H$ group.[58] Moreover, the bands at 1488 and 1541 cm^{-1} were assigned to adsorbed pyridine on both Lewis and Brønsted acid sites[59] and pyridinium ions (PyH^+) formed on Brønsted acid sites,[60] respectively. This evidence confirmed that the surface of CBSA had Brønsted acid sites, which were needed for the catalytic dehydration of fructose to 5-HMF.

3.2 Catalytic performance testing

The catalytic activities for fructose conversion to 5-HMF of CBSA in a DMSO monophasic solvent system at reaction temperatures of 100 °C, 120 °C, and 140 °C for 45, 120, and 180 min with a 10 wt% catalyst loading are shown in Fig. 3. For the reaction time of 45 min, it was observed that the fructose conversion increased with increasing reaction temperature (Fig. 3a). A similar trend was observed for reaction times of 120 and 180 min. Moreover, at the reaction temperature of 140 °C, nearly complete or complete conversion of fructose (98–100%) occurred for all the studied reaction times. Fig. 3b illustrates the effects of reaction temperature and reaction time on the 5-HMF yield for the CBSA-catalyzed conversion of fructose to 5-HMF. For reaction times of 45, 120, and 180 min, the obtained 5-HMF yield increased from 32% to 80%, 64% to 82%, and 71% to 85%, respectively, as the reaction temperature was increased from 100 °C to 140 °C. Noticeably, the variation in reaction time at 140 °C did not significantly affect the yield of 5-HMF. Nevertheless, the reaction time of 180 min was selected as the optimized reaction time. This was because the highest 5-HMF yield, *ca.* 85%, was obtained when the reaction was allowed to proceed for 180 min. According to the published reports on fructose conversion to 5-HMF in DMSO, the remaining total yield of 15% under the optimal reaction conditions (*i.e.*, 140 °C and 180 min) could be attributed to humins, which are products formed from the polymerization or cross-polymerization of 5-HMF and/or fructose.[24,61–63] The formation of 5-HMF from fructose in the absence of CBSA was also studied. The results showed that a 5-HMF yield of only 2% was obtained when the reaction was performed at 140 °C for 45 min without the CBSA catalyst. Compared with the 5-HMF yield of 80% obtained when the reaction was performed under the same reaction conditions with CBSA, the significantly higher 5-HMF yield corroborated the catalytic effect of CBSA on the conversion of fructose to 5-HMF. As shown in Fig. 3c, at reaction temperatures higher than 100 °C, the selectivities for 5-HMF were similar. In other words, the reaction time had only a minor influence on 5-HMF selectivity when the reaction temperature was greater than 100 °C. On the other hand, when the reaction was allowed to proceed at 100 °C, an increase in the reaction time from 45 min to 120 min

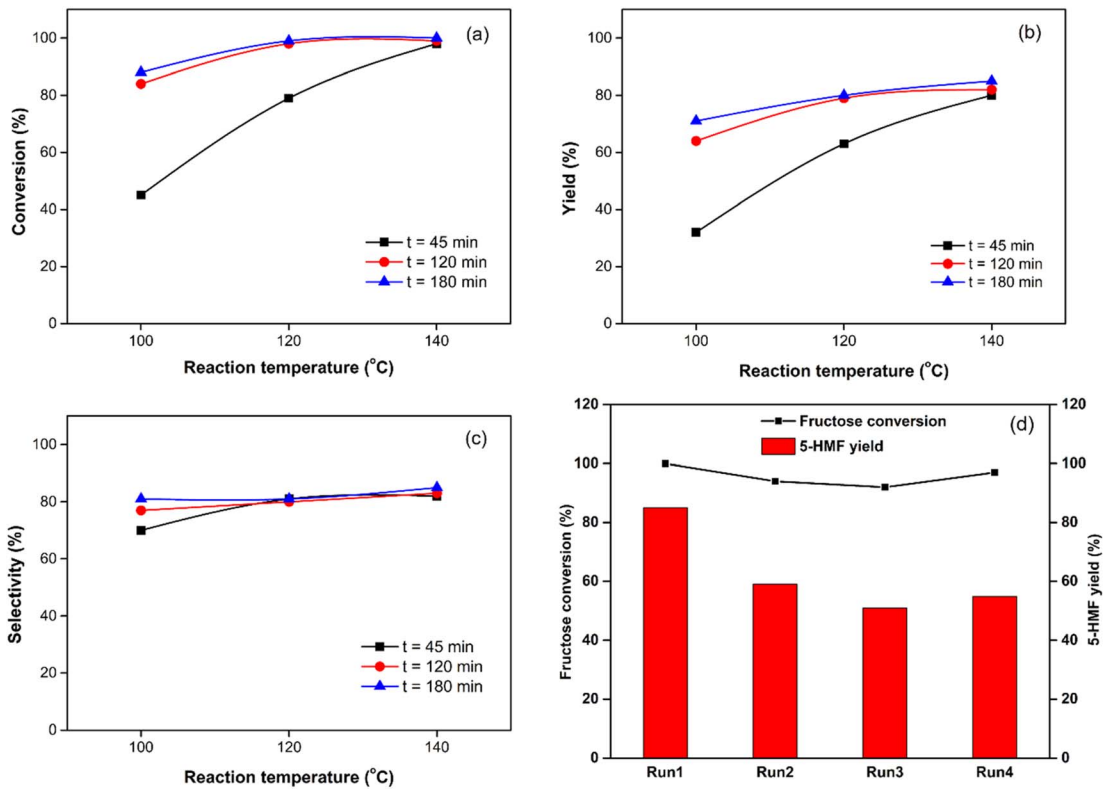

Fig. 3 Catalytic activity of CBSA for the conversion of fructose to 5-HMF at reaction temperatures ranging from 100–140 °C and reaction times of 45 min, 120 min, and 180 min: (a) conversion of fructose, (b) yield of 5-HMF, (c) selectivity of 5-HMF, and (d) CBSA reusability test at 140 °C, 180 min, and an initial N_2 pressure of 5 bar.

resulted in a drastic increase in the selectivity of 5-HMF. Further increasing the reaction time to 180 min resulted in only a slight improvement in the selectivity of 5-HMF. The highest 5-HMF selectivity of approximately 85% for the 10 wt% CBSA-catalyzed fructose conversion to 5-HMF was obtained when the optimal reaction conditions were employed.

It is widely known that cellulose under acidic conditions and high temperatures can undergo thermal degradation to form products, such as glucose, levoglucosan, oligomers, and 5-HMF. Since this crucial point was already well established, a controlled experiment with only CBSA and the DMSO solvent was conducted. The total solid weight loss was found to be 8%, with no detection of glucose or 5-HMF, the two potential cellulose degradation products. Nevertheless, it was likely that the cellulose within the catalyst could have undergone degradation to some extent, producing products such as levoglucosan and/or oligomers under the employed reaction conditions. Minimizing catalyst loss will thus be a key focus for further investigations.

The optimized catalytic activity of CBSA for the conversion of fructose to 5-HMF was compared to that of other bio-based catalysts, and the comparison is shown in Table 1. It can be seen from the table that CBSA exhibited promising catalytic performance for the fructose conversion to 5-HMF in DMSO-based solvent systems, with a relatively low catalyst dosage and acid density of 10 wt% and 0.21 $mmol_{-SO_3H}$ per gram CBSA, respectively. Unlike other bio-based acid catalysts, the benzenesulfonic acid (–$PhSO_3H$), rather than the conventional sulfo (SO_3H) functional group, was anchored to the base material for CBSA. It was therefore asserted that the benzenesulfonic acid group was also capable of catalyzing the dehydration of fructose to produce 5-HMF. Compared with the use of carbon materials derived from the carbonization of biomass or biomass-derived compounds at high temperatures,[24,27,33] the direct utilization of cellulose for the preparation of a solid acid catalyst could be more beneficial in terms of energy consumption. Since the preparation of CBSA does not require the use of chlorosulfonic acid[18] or a corrosive sulfuric acid sulfonating agent,[27,33] using CBSA as a solid acid catalyst for the conversion of fructose to 5-HMF is of great interest. Although DMSO has been demonstrated to be an excellent solvent for 5-HMF production from carbohydrates, its strong affinity for 5-HMF causes difficulty in product separation and purification. To overcome this challenge, attempts have been made to search for solvent systems which are capable of producing HMF in exceptionally high yields and could be easily separated from 5-HMF. The biphasic solvent systems, which consist of a reaction phase and an extraction phase, have shown promising capability to meet those requirements. Olivito *et al.* reported the use of biphasic solvent systems with rare earth metal triflate catalysts for glucose and fructose conversion to 5-HMF. Interestingly, an impressively high 5-HMF yield of 99% was obtained from fructose in a methyl propyl ketone (MPK)/$Sc(OTf)_3$/choline chloride biphasic system at 150 °C.[64] Zhang *et al.* achieved a 62.9% 5-HMF yield from untreated wheat straw in a THF/H_2O + NaCl saturated two-phase system with a catalyst combination of $FePO_4$ and mandelic acid. These findings provide new

Table 1 Comparison of the reactivities of some previously reported bio-based catalysts for the catalytic conversion of fructose to 5-HMF

Entry	Catalyst	Catalyst dosage[a] (wt%)	Solvent	Reaction temperature (°C)	Total acid density[b] (mmol g^{-1})	Acid density[b] ($mmol_{-SO_3H}$ g^{-1})	Conversion (%)	5-HMF yield (%)	Ref.
1	Cellulose sulfuric acid (cellulose-based)	28	DMSO	100	0.54	0.54	100	93.6	18
2	LCSA-900 (carbon-based)	150	DMSO	170	0.88	0.88	98.0	75.7	33
3	SAC-4-2-SO_3H (carbon-based)	50	Acetone/DMSO mixture (volume ratio: 8/2)	130	4.44	1.38	99	90	27
4	LDMCC-900 (carbon-based)	10	DMSO	140	2.4[c]	N/A[d]	98.9	74.3	24
5	LDMCC-900 (carbon-based)	10	DMSO	180	2.4[c]	N/A[d]	100	96.0	24
6	Scandium(III) triflate ($Sc(OTf)_3$)	4[e]	Choline chloride	150	N/A	N/A	100	99	64
7	CBSA (cellulose-based)	10	DMSO	140	N/A[d]	0.21	100	85	This work

[a] Catalyst dosage is expressed in wt% with respect to the weight of fructose used. [b] The reported acid density values were determined by acid–base titration. [c] mmol of –COOH per gram catalyst. [d] N/A = not available. [e] In molar quantity.

insights for further investigation of the CBSA-catalyzed dehydration of fructose to 5-HMF, especially the development of biphasic solvent systems.[65]

3.3 Catalyst reusability and investigation of the spent catalyst

Catalyst reusability is considered an important requirement for the use of heterogeneous catalysts. In this study, the catalytic activity of the spent catalysts, namely CBSA-1, CBSA-2, and CBSA-3, for the conversion of fructose to 5-HMF was examined. It was found that all the spent catalysts exhibited lower catalytic activity than the as-synthesized CBSA, as shown in Fig. 3d. The fructose conversion decreased to 94% when CBSA-1 was used. The conversion of fructose slightly decreased in run 3 but increased to 97% in run 4. In terms of the 5-HMF yield, a moderate decrease from 85% to 59% was observed after one reuse cycle. Also, the 5-HMF yield showed only slight changes after the 2nd and 3rd reuse cycles compared with that obtained from run 2 with CBSA-1.

The spent catalyst obtained after the fourth run, referred to as CBSA-4, was characterized by FTIR, PXRD, and XPS techniques (Fig. 4). The FTIR spectrum of CBSA-4 was similar to that of CBSA (Fig. 4a), indicating an analogy in the chemical structures of both catalysts. The absence of the IR peaks centered at approximately 1033 and 1005 cm^{-1} for CBSA-4 could be due to peak overlapping. Two new pronounced peaks centered at 1019 and 950 cm^{-1} were observed in the spectrum of CBSA-4. These two IR absorption bands, corresponding to the stretching vibration of S=O bond in DMSO-containing adducts, could be hypothetically attributed to the insoluble compounds bearing DMSO.[66,67] The PXRD pattern of CBSA-4, as shown in Fig. 4b, displayed a single broad peak at $2\theta = 22°$, indicating that amorphous regions were still predominant in the spent catalyst. Next, the XPS analysis of CBSA-4 was conducted, and the results are shown in Fig. 4c, S2c, d and Table S1.† The high-resolution S 2p spectrum was deconvoluted into three distinct doublets at different binding energies (see Fig. 4c). The binding energy of the S $2p_{3/2}$ core-level electron at 168.0 eV, characteristic of the $-SO_3H$ group, could not be observed, indicating a decrease in the sulfo groups, possibly due to the desulfonation of benzenesulfonic acid in the presence of water and acidic protons. Instead, a peak was observed at 168.9 eV, associated with the oxidized forms of sulfur (SO_x).[68] Moreover, the main peak was shifted to a lower binding energy of 163.7 eV, suggesting the formation of reduced forms of sulfur, such as thiol (–SH) groups.[68,69] Considering the characterization results of

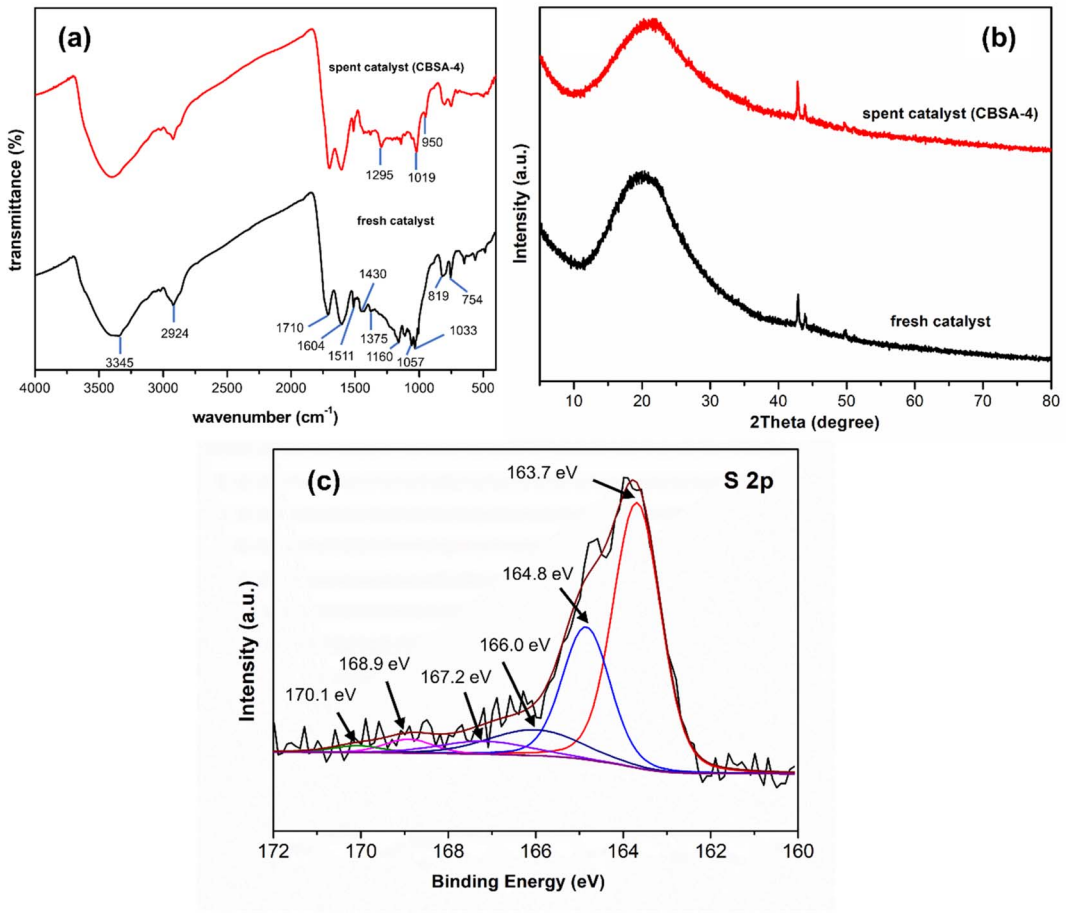

Fig. 4 Characteristics of the as-synthesized and spent CBSA catalysts. (a) FTIR spectra, (b) PXRD patterns of fresh CBSA and CBSA-4, and (c) XPS spectrum of CBSA-4.

CBSA-4, the decrease in catalytic activity was mainly ascribed to the decline in the $-SO_3H$ groups, which were the active sites for the catalytic dehydration of fructose. This conclusion was corroborated by the determined number of $-SO_3H$ groups of 0.034 mmol g_{sample}^{-1} for the CBSA-4 spent catalyst. Ignatyev *et al.* studied the synthesis of glucose esters from cellulose in ionic liquids. Their study focused on the synthesis of α-D-glucose pentaacetate (GPAc) from cellulose *via* an Amberlyst 15Dry acid-catalyzed hydrolysis and acetylation.[70] They found that the sulfonic acidity of Amberlyst 15Dry was leached during the hydrolysis reaction, and a similar situation was observed in this work. The recyclability test revealed that a similar high yield of GPAc to that attained after the first reaction cycle could be obtained with the H_2SO_4 solution-regenerated Amberlyst 15Dry. This approach could be useful for restoring the activity of the spent CBSA catalysts for the conversion of fructose to 5-HMF.

4. Conclusion

Cellulose benzenesulfonic acid (CBSA) was successfully synthesized by reacting cellulose microcrystal (CMC) powder with 4-chlorobenzenesulfonic acid in toluene. The obtained CBSA product was mainly amorphous and thermally stable under a N_2 atmosphere up to 150 °C. The optimal reaction conditions for the conversion of fructose to 5-HMF in DMSO were 140 °C and 180 min. The highest 5-HMF yield of 85% and fructose conversion of 100% were achieved with a 10 wt% loading of CBSA. The recyclability test demonstrated that the fresh CBSA catalyst exhibited higher catalytic activity than the spent catalysts. After the third reuse cycle (fourth run), the activity dropped to a 55% HMF yield with a fructose conversion of 97%. According to the characteristics of the spent catalyst (CBSA-4), it is most likely that an inadequate amount of $-SO_3H$ was responsible for the performance loss observed in the reusability study.

Data availability

The authors confirm that the data supporting the findings of this study are available within the article and the ESI.† Additional data that support the findings of this study are available from the corresponding author upon reasonable request.

Author contributions

A. P. contributed to the concept and design of the research, preparation, characterization, and analysis of cellulose, catalytic performance testing, and the original draft of the manuscript. A. S. contributed to reviewing and editing the final manuscript. V. I. contributed to the concept and design of the research, supervision, visualization, funding acquisition, and reviewing and editing the final manuscript. All authors have approved the final version of the manuscript.

Conflicts of interest

The authors declare no conflicts of interest.

Acknowledgements

This work was supported by the National Research Council of Thailand (NRCT) under contract no. NRCT5-RSA63026-01 to V. I. and the National Science and Technology Development Agency (NSTDA) (P2051917). The authors would like to thank Ms Surisa Kongthong and Assistant Professor Dr Junjuda Unruangsri for the NMR measurements and valuable discussions.

References

1 J. Dai, Z. Liu, Y. Hu, S. Liu, L. Chen, T. Qi, H. Yang, L. Zhu and C. Hu, *Catal. Sci. Technol.*, 2019, **9**, 483–492.
2 J. Chuseang, V. Itthibenchapong, A. Srifa, W. Praikaew, S. Tuntithavornwat, B. Rungtaweevoranit, S. Ratchahat, W. Koo-Amornpattana, W. Klysubun, A. Eiad-ua, W. Kiatkittipong and S. Assabumrungrat, *ChemCatChem*, 2023, **15**, e202300543.
3 L. Atanda, M. Konarova, Q. Ma, S. Mukundan, A. Shrotri and J. Beltramini, *Catal. Sci. Technol.*, 2016, **6**, 6257–6266.
4 K. Sun, Y. Shao, Q. Li, L. Zhang, Z. Ye, D. Dong, S. Zhang, Y. Wang, X. Li and X. Hu, *Catal. Sci. Technol.*, 2020, **10**, 2293–2302.
5 D.-M. Gao, B. Zhao, H. Liu, K. Morisato, K. Kanamori, Z. He, M. Zeng, H. Wu, J. Chen and K. Nakanishi, *Catal. Sci. Technol.*, 2018, **8**, 3675–3685.
6 S. Zhang, Z. Zheng, C. Zhao and L. Zhang, *ACS Omega*, 2017, **2**, 6123–6130.
7 X. Hou, Y. Zhong, J. Xiao, J. Wang, J. Cai, Z. Zeng, S. Deng and Q. Deng, *AIChE J.*, 2023, **69**, e18047.
8 A. D. French, *Cellulose*, 2017, **24**, 4605–4609.
9 B. Zheng, S. Yu, Z. Chen and Y.-X. Huo, *Front. Microbiol.*, 2022, **13**, 933882.
10 P. Hu, Y. Hu, H. Li, L. Li, Z. Xue, D. Wu, J. Zhao, C. Hu and L. Zhu, *Carbohydr. Polym.*, 2023, **309**, 120692.
11 A. M. Raspolli Galletti, R. Lorè, D. Licursi, N. Di Fidio, C. Antonetti and S. Fulignati, *Catal. Today*, 2023, **418**, 114054.
12 F. Shi, J. Wang, H. Wang, C. Liu, Y. Lu, X. Lin, D. Hou, C. Wen, S. Yang, C. Luo, Z. Zheng and Y. Zheng, *J. Energy Inst.*, 2023, **108**, 101206.
13 K. Enomoto, T. Hosoya and H. Miyafuji, *Cellulose*, 2018, **25**, 2249–2257.
14 T. Huang, Y. Zhou, X. Zhang, D. Peng, X. Nie, J. Chen and W. Xiong, *Cellulose*, 2022, **29**, 1419–1433.
15 B. Maleki, R. Sandaroos, S. Naderi and S. Peiman, *J. Organomet. Chem.*, 2023, **990**, 122666.
16 X. Liu and F. Liu, *Carbohydr. Polym.*, 2023, **310**, 120726.
17 R. M. d. R. Santana, D. C. Napoleão, J. M. Rodriguez-Diaz, R. K. d. M. Gomes, M. G. Silva, V. M. E. d. Lima, A. A. d. Melo Neto, G. M. Vinhas and M. M. M. B. Duarte, *Chemosphere*, 2023, **326**, 138453.
18 B. Liu, Z. Zhang and K. Huang, *Cellulose*, 2013, **20**, 2081–2089.
19 M. A. Nasseri, M. Salimi and A. A. Esmaeili, *RSC Adv.*, 2014, **4**, 61193–61199.

20 Z. Daneshfar and A. Rostami, *RSC Adv.*, 2015, **5**, 104695–104707.
21 A. Rezayan, Y. Zhang, B. Li and C. C. Xu, *ChemCatChem*, 2023, **15**, e202300973.
22 S. Pumrod, A. Kaewchada, S. Roddecha and A. Jaree, *RSC Adv.*, 2020, **10**, 9492–9498.
23 W. Fang and A. Riisager, *ChemCatChem*, 2024, **16**, e202400394.
24 S. Wang, T. L. Eberhardt and H. Pan, *Fuel*, 2022, **316**, 123255.
25 K.-L. Chang, S. C. Muega, B. I. G. Ofrasio, W.-H. Chen, E. G. Barte, R. R. M. Abarca and M. D. G. de Luna, *Chemosphere*, 2022, **291**, 132829.
26 X. Kong, S. Vinju Vasudevan, M. Cao, J. Cai, H. Mao and Q. Bu, *ACS Sustain. Chem. Eng.*, 2021, **9**, 15344–15356.
27 H. Liu, Q. Peng, J. Ren, B. Shi and Y. Wang, *J. Iran. Chem. Soc.*, 2021, **18**, 2649–2656.
28 A. D. K. Deshan, J. J. Forero, J. P. Bartley, C. Marasinghege, K. Tuiatua, J. Beltramini and W. O. S. Doherty, *Fuel*, 2021, **306**, 121670.
29 X. Lyu, H. Li, H. Xiang, Y. Mu, N. Ji, X. Lu, X. Fan and X. Gao, *Chem. Eng. J.*, 2022, **428**, 131143.
30 G. T. T. Le, K. Arunaditya, J. Panichpol, T. Rodruangnon, S. Thongratkaew, K. Chaipojjana, K. Faungnawakij and T. Charinpanitkul, *Catal. Commun.*, 2021, **149**, 106229.
31 M. Nasrollahzadeh, N. S. S. Bidgoli, N. Shafiei and F. Momenbeik, *Int. J. Biol. Macromol.*, 2021, **182**, 59–64.
32 Y. Hu, M. Li, Z. Gao, L. Wang and J. Zhang, *Mater. Today Chem.*, 2021, **20**, 100423.
33 M. Li, Q. Zhang, B. Luo, C. Chen, S. Wang and D. Min, *Ind. Crops Prod.*, 2020, **145**, 111920.
34 G. Portillo Perez and M.-J. Dumont, *Chem. Eng. J.*, 2020, **382**, 122766.
35 X. Wang, Q. Deng, Y. Zhang, Z. Ren and P. He, *Res. Chem. Intermed.*, 2023, **49**, 1369–1386.
36 M. Zuo, Q. Niu, Y. Zhu, S. Li, W. Jia, Z. Zhou, X. Zeng and L. Lin, *Ind. Crops Prod.*, 2023, **192**, 115953.
37 H. Li, Q. Deng, H. Chen, X. Cao, J. Zheng, Y. Zhong, P. Zhang, J. Wang, Z. Zeng and S. Deng, *Appl. Catal., A*, 2019, **580**, 178–185.
38 Q. Zhang, P. Jiang, Z. Nie and P. Zhang, *New J. Chem.*, 2020, **44**, 1588–1593.
39 N. Fairley, V. Fernandez, M. Richard-Plouet, C. Guillot-Deudon, J. Walton, E. Smith, D. Flahaut, M. Greiner, M. Biesinger, S. Tougaard, D. Morgan and J. Baltrusaitis, *Applied Surface Science Advances*, 2021, **5**, 100112.
40 J. Zhao, C. Zhou, C. He, Y. Dai, X. Jia and Y. Yang, *Catal. Today*, 2016, **264**, 123–130.
41 L. Tang, B. Huang, Q. Lu, S. Wang, W. Ou, W. Lin and X. Chen, *Bioresour. Technol.*, 2013, **127**, 100–105.
42 L. Pachuau, *J. Appl. Pharm. Sci.*, 2014, **4**, 87–94.
43 M. K. Haafiz, A. Hassan, Z. Zakaria and I. Inuwa, *Carbohydr. Polym.*, 2014, **103**, 119–125.
44 F. Jiang and Y.-L. Hsieh, *Carbohydr. Polym.*, 2015, **122**, 60–68.
45 T. Narkkun, W. Kraithong, S. Ruangdit, C. Klaysom, K. Faungnawakij and V. Itthibenchapong, *ACS Omega*, 2023, **8**, 45428–45437.
46 J. X. Leong, W. Wan Daud, A. Ahmad, M. Ismail and B. Liew, *Int. J. Hydrogen Energy*, 2015, **40**, 11604–11614.
47 J. Coates, in *Encyclopedia of Analytical Chemistry*, 2006, DOI: **10.1002/9780470027318.a5606**.
48 A. Sasaki, T. Konishi, K. Kobayashi, M. Wada and R. Kusumi, *Cellulose*, 2024, **31**, 7895–7904.
49 J. Gong, J. Li, J. Xu, Z. Xiang and L. Mo, *RSC Adv.*, 2017, **7**, 33486–33493.
50 V. Deerattrakul, P. Sakulaue, A. Bunpheng, W. Kraithong, A. Pengsawang, P. Chakthranont, P. Iamprasertkun and V. Itthibenchapong, *Electrochim. Acta*, 2023, **453**, 142355.
51 D. Ciolacu, F. Ciolacu and V. Popa, *Cellul. Chem. Technol.*, 2011, **45**, 13–21.
52 P. K. Chatterjee and C. M. Conrad, *Journal of Polymer Science, Part A-1: Polymer Chemistry*, 1968, **6**, 3217–3233.
53 F. Barroso-Bujans, J. L. G. Fierro, S. Rojas, S. Sánchez-Cortes, M. Arroyo and M. A. López-Manchado, *Carbon*, 2007, **45**, 1669–1678.
54 A. Aldana-Pérez, L. Lartundo-Rojas, R. Gómez and M. E. Niño-Gómez, *Fuel*, 2012, **100**, 128–138.
55 T. C. Tudino, R. S. Nunes, D. Mandelli and W. A. Carvalho, *Front. Chem.*, 2020, **8**, 263.
56 J. Araujo, B. Archanjo, K. de Souza, W. Kwapinski, N. Falcão, E. Novotny and C. Achete, *Biol. Fertil. Soils*, 2014, **50**, 1223–1232.
57 I. Pełech, U. Narkiewicz, D. Moszyński and R. Pełech, *J. Mater. Res.*, 2012, **27**, 2368–2374.
58 P. P. Upare, J.-W. Yoon, M. Y. Kim, H.-Y. Kang, D. W. Hwang, Y. K. Hwang, H. H. Kung and J.-S. Chang, *Green Chem.*, 2013, **15**, 2935–2943.
59 A. I. Osman, J. K. Abu-Dahrieh, D. W. Rooney, S. A. Halawy, M. A. Mohamed and A. Abdelkader, *Appl. Catal., B*, 2012, **127**, 307–315.
60 I. Khalil, C. M. Celis-Cornejo, K. Thomas, P. Bazin, A. Travert, D. J. Pérez-Martínez, V. G. Baldovino-Medrano, J. F. Paul and F. Maugé, *ChemCatChem*, 2020, **12**, 1095–1108.
61 R. Tomer and P. Biswas, *New J. Chem.*, 2020, **44**, 20734–20750.
62 H. Cai, C. Li, A. Wang, G. Xu and T. Zhang, *Appl. Catal., B*, 2012, **123–124**, 333–338.
63 J. C. Velasco Calderon, J. S. Arora and S. H. Mushrif, *ACS Omega*, 2022, **7**, 44786–44795.
64 F. Olivito, V. Algieri, M. A. Tallarida, A. Jiritano, P. Costanzo, L. Maiuolo and A. D. Nino, *Green Chem.*, 2023, **25**, 1679–1689.
65 X. Zhang, H. Cui, Q. Li and H. Xia, *Energy Fuels*, 2023, **37**, 12953–12965.
66 W. Zhang, Y. Jiang, Y. Ding, M. Zheng, S. Wu, X. Lu, X. Gao, Q. Wang, G. Zhou, J. Liu, M. J. Naughton, K. Kempa and J. Gao, *Opt. Mater. Express*, 2017, **7**, 2150–2160.
67 I. Wharf, T. Gramstad, R. Makhija and M. Onyszchuk, *Can. J. Chem.*, 1976, **54**, 3430–3438.
68 G. Gabka, P. Bujak, K. Kotwica, A. Ostrowski, W. Lisowski, J. Sobczak and A. Pron, *Phys. Chem. Chem. Phys.*, 2017, **19**, 1217–1228.
69 L. J. Konwar, A. Samikannu, P. Mäki-Arvela, D. Boström and J.-P. Mikkola, *Appl. Catal., B*, 2018, **220**, 314–323.
70 I. Ignatyev, P. Mertens, K. Binnemans and D. De Vos, *Holzforschung*, 2012, **66**, 417–425.